



Technical Sciences  
Academy of Romania  
[www.jesi.astr.ro](http://www.jesi.astr.ro)

## Journal of Engineering Sciences and Innovation

Volume 8, Issue 1 / 2023, pp. 31-42

<http://doi.org/10.56958/jesi.2023.8.1.31>

**C. Chemical Engineering, Materials Science and  
Engineering**

Received 17 November 2022

Accepted 24 March 2023

Received in revised form 23 February 2023

### Evaluation of abrasive wear resistance of self-fluxing Ni-base coatings by scratch testing

MUNTEANU C.<sup>1,3</sup>, CHICET D.L.<sup>1\*</sup>, ISTRATE B.<sup>1</sup>, BENCHEA M.<sup>1</sup>,  
PAULIN C.<sup>1</sup>, VIDA-SIMITI I.<sup>2,3</sup>

<sup>1</sup>"Gheorghe Asachi" Technical University of Iași, Bd. D. Mangeron 6, 700050 Iași, Romania

<sup>2</sup>Technical University of Cluj-Napoca, 103-105 Muncii Ave., Cluj-Napoca, 400641, Romania

<sup>3</sup>Technical Sciences Academy of Romania, 26 Dacia Blvd, Bucharest, 030167, Romania

**Abstract.** Abrasion wear is one of the most dominant types of wear in many applications, causing over 50% of all wear failures [1]. The abrasive wear phenomenon could be classified regarding several aspects: a) the position of the abrasive particles: two-body abrasion if they are fixed, or three-body abrasion if they are free to slide and/or roll, b) the stresses involved: gouging abrasion, high-stress abrasion (grinding) and low-stress abrasion (scratching), c) the surface appearance: ploughing, cutting, fatigue and fracture (cracking). In this study was approached the possibility of abrasion wear resistance evaluation of self-fluxing Ni-base coatings by scratch testing. Materials used in tests were: three self-fluxing Ni-base coatings deposited on low-alloyed steel substrate using flame spraying process (referred to as S1, S2 and S3). The wear of the samples and the friction coefficient were investigated with scratch tester and analyzed in correlation with their mechanical properties.

**Keywords:** abrasive wear, NiCrBSi coating, scratch test.

#### 1. Introduction

The coatings manufactured by thermal spraying technique are used for decades and begin to earn their rightful place in various fields of industry, being used in order to improve wear resistance, corrosion, thermal stresses etc.

For this reason, is necessary to find a more accurate and rapid characterization of parameters that influence the coatings quality, the most important being: porosity,

---

\*Correspondence address: [dchicet@tuiasi.ro](mailto:dchicet@tuiasi.ro)

microstructure, thickness, unmelted particles presence, oxides and cracks, microhardness and bond strength [1, 2, 32].

All these parameters determine the sustainability of a coating by the influence they have on the quality of the adhesion on substrate, and cohesion between splats forming layer.

One of the most important types of wear encountered in many applications of thermal spray coatings is abrasive wear. It is even considered that more than 50% of malfunctions cases are caused by abrasive wear [3].

The major problem brought by the appearance of such a phenomenon is related to the costs involved in remediation and replacement of worn parts, the machine residence time and high cost of maintenance, if the phenomenon occurs with a high frequency.

The phenomenon of abrasive wear can be classified according to several aspects: position abrasive particles, surface tension and appearance waste products. In the first case, abrasive wear processes are classified as: abrasion between two bodies (if abrasive particles are fixed), or abrasion between three bodies (if abrasive particles have a sliding or rolling free movement in the production of wear).

In the second case, the classification according to the tensions involved, there are four categories: 1. gouging abrasion - is characterized by very high stresses that lead to a generalized plastic deformation of materials, producing large dimples on the surface after detachment and removal of large abrasive particles from the surface. 2. high stress abrasion is characterized by the occurrence of different degrees of scratching on the surface, caused by abrasive particles broken from worn layer. These particles appear after chipping or by plastic deformation of surface elements caused by the fatigue phenomenon. 3. Low stress abrasion is characterized by the appearance of fine scratching traces, because of loads are not so great as to produce uprooting of abrasive particles on the surface subjected to solicitation. [4, 5]

The third aspect that occurs in the classification of abrasive wear phenomenon is the appearance of the surface after removing abrasive factors, thus observed four categories: plowing, cutting, fatigue and fracture (cracking). [6].

Abrasive wear resistance of materials can be determined by several laboratory methods, standardized or non-standardized [7-13], which however cannot reproduce all requests faced when operating. One of these tests, non-standardized yet, is the scratch test, used for many years in order to evaluate the scratch resistance of a material and, more recently, in order to evaluate the adhesion of a coating to the substrate [14-19], purpose for it was standardized [20].

Using scratch test for evaluating the resistance to abrasive wear derives itself from its production mechanism: cumulative actions of scratching produced by a large number of abrasive particles or high hardness asperities [21]. In practice, this method is often used for checking the quality of surfaces compared to other known properties, in a short time and with good repeatability.

The method itself consists in pressing a sharp tip on the surface tested until the damage occurs, at a critical load ( $L_c$ ). Failure appearance of the layer can be

different: peeling of the coat, deep cracks, plastic deformation or cracking of the coating / substrate [22-25].

Failure types occurred in case of the scratch tests depends on many factors: intrinsic (loading rate, scratching speed, type indenter radius, indenter wear [16, 26, 27] or extrinsic (substrate properties: hardness, elastic modulus, coating properties: thickness, hardness modulus, residual stress, friction coefficient, surface roughness [16, 28, 27].

Some studies have shown that the failure modes can be characterized easier depending on the hardness of the deposited layer and the substrate [26] and the type of material deformation, which can be ductile or brittle.

Thus, there can be described four cases. Soft substrate – soft coatings, when the failure is mainly plastic deformation and groove formation, with small cracks observed only at very high loads. Soft substrate – hard coatings, when the predominant failure of substrate is plastic deformation and fracture or plastic deformation of the coating. On harder substrate – soft coatings case, the coatings suffer some plastic deformation and extrusion between the indenter tip and the substrate. For hard substrates with hard coatings, the main failure type is fracture of coatings, whilst the plastic deformation is minimal. Hard coatings were considered the ones with hardness greater than 5 GPa.

As mentioned before, the failure modes of hard coatings can be classified into four categories [26].

1. *through – thickness cracking*: the cracks are stopped at the interface with the substrate but may extend into substrate when it is brittle. It includes tensile cracking behind the indenter, Hertzian cracking and conformal cracking when coating is bent into the scratch scar. [23, 30]
2. *coating detachment*: compressive spallation or buckling spallation in front of the indenter tip, or elastic recovery – induced spallation behind indenter tip [23, 30]
3. *chipping within the coating*: could be observed in the case of thick coatings on a softer substrate [29].
4. *chipping within the substrate*: in case of hard/brittle coatings, with very good adherence on hard substrates, the system tends to behave as bulk; if the coating is very thin, the chipping of substrate can occur.

As aforementioned, another very important parameter in case of scratch test is the loading force that acts between indenter tip (which simulates abrasive particle action) and the wear tested surface. Thus, the scratch tests can be differentiated into: high stress abrasion (characterized by high loads that produce considerable fracture to the material) and low-stress abrasion (when the loads are lower and less fracture damage is caused). [31]

In the present paper, the possibility of the abrasive wear resistance of self-fluxing Ni-base coatings evaluation by scratch tests was studied. The materials used in the tests were three Ni-base self-fluxing coatings deposited on a low-alloyed steel substrate via flame-spray method. The scratch tests were conducted both on the surface (as usually) and on the cross-section of the coatings (method proposed

recently to evaluate the adhesion/cohesion of thick thermal sprayed coatings [6, 11, 12, 13].

## 2. Materials and methods

### 2.1. Materials

Three Ni-base self-fluxing powders were used in the experiment as feedstock materials: 1060-00 type powder and 1355-20 powder type (manufactured by Hognas) and JK-586 powder type (manufactured by Deloro Stellite Co). The chemical compositions of sprayed powders are listed in Table 1.

Table 1. Chemical composition of Ni-base self-fluxing powders

Chemical composition	% Ni	% Cr	% Si	% B	% Fe	% C	% Mo	% Cu
1060-00	73	14.92	4.31	3.17	3.82	0.78	-	-
1355-20	67.47	15.8	4.07	3.49	2.72	0.54	2.96	2.95
JK-586	72.9	15	4.3	3.1	4	0.7	-	-
Steel	-	-	0.22	-	bal	0.34	-	-

The powders are Ni-base self-fluxing alloys, characterized by a melting point around 1000°C. Figure 1 presents the typical scanning electron microscopy photography of two powders, along with the chemical analysis (both conducted on SEM-EDX microscope Quanta 200-3D type, FEI).

As it can be observed, all the powders showed a spherical morphology, being characterized by a particle size range of 20-60 µm (in case of 1060 powder) and 40-80µm (in case of 1355 and JK586 powders). The substrate material for all three coatings was a low-alloyed steel (see the chemical composition in Table 1), which was not subject to any thermal treatment. The substrate was prepared as lamellas of 80x10x3 mm.

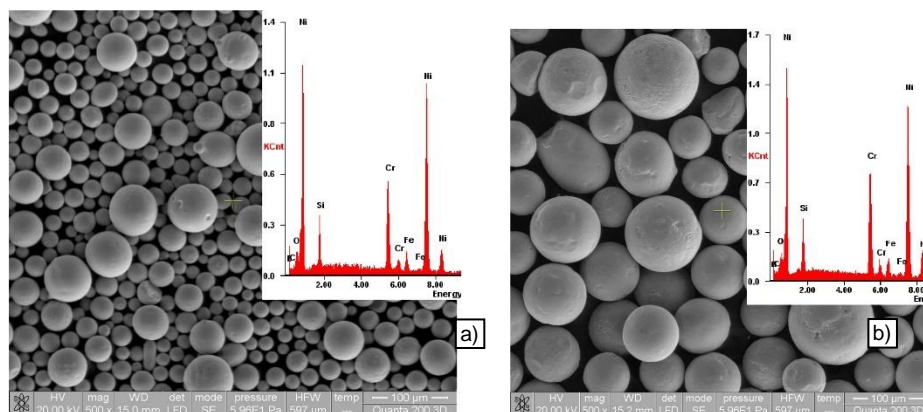


Fig. 1. Typical SEM images of powder morphology and EDX spectrum for: a)1060-00 powder, b) JK-586 powder.

## **2.2. Coating deposition**

The coatings were produced using the flame-spray method. Before the spraying operations, the low-alloyed steel samples were degreased with acetone and alcohol and grit blasted with corundum particles, in order to obtain a rust and impurity-free surface, with a mean roughness of 1  $\mu\text{m}$ . The roughing activation operation is mandatory because allows mechanical bonding between the substrate and the coating. The samples were placed on a holding system and subjected to thermal spraying.

The flame-spraying process was carried-out using neutral flame of oxy-acetylene gas, with the oxygen pressure of 3 – 4 bar and acetylene pressure of 0,7 – 1,5 bar. Others parameters of the thermal spray process were: temperature reached at deposition of 1000°C, distance between torch tip and substrate of 20 cm, preheating temperature of substrate of 50 – 80 °C. After the coatings were manufactured, they were subjected to fusing by flame remelting, in order to obtain a metallurgical bond with the substrate. This operation consisted of applying an oxy-acetylene flame to the coating till the fusing temperature was reached (800°C in this case), maintained for few minutes and slow-cooled in air.

## **2.3. Microstructures and mechanical properties**

The coated samples were cut using abrasive disc water-cooled and were cold-mounted in polyester resin, for the scratch tests conducted on coating cross-section. The samples for both scratch tests were polished following standard metallographic techniques and finished (using abrasive suspension) to achieve a mean roughness of  $R_a = (0,12 - 0,15) \mu\text{m}$ .

The microstructure was analyzed using a scanning electron microscope Quanta 200-3D type, produced by FEI, Eindhoven, Netherland, which has an integrated chemical-analysis module EDX-type, produced by EDAX-AMETEK, Netherland. Microindentation tests were carried out on the Microtribometer UMTR 2M-CTR, with a diamond indenter tip at 120° and a radius of 0,2  $\mu\text{m}$ , with a maximum load of 20N.

## **2.4. Scratch tests**

Both scratch tests were performed according to standards, under dry sliding conditions, in ambient air at room temperature and 30% humidity, on the Microtribometer UMTR 2M-CTR, using an indenter DFH-20 Dual Friction/Load sensor type, which has a tungsten carbide microblade with a radius of 0,4mm.

The scratch tests of the surfaces were carried out with PLST (Progressive Loading Scratch Test) when the normal load was increased linearly during the test from 0 to 20N, test duration was fixed at 1 min, the speed of the indenter was preset at 10 mm/min and for each sample three scratches were made. After the tests, the scratch scars were observed using both an optic microscope (at 20x) and SEM (HV = 20kV, 100x, WD = 15mm, ETDetector). The end of scratch scars (corresponding to the maximum load) was analyzed using the EDS module (line-chemical analysis).

The profile of the scratch scars was recorded using the system Form Talysurf Intra (Taylor-Hobson, Leicester, England).

The scratch tests were conducted on the coating cross-section with CLST (Constant Loading Scratch Test) when the indenter moved from the steel substrate through the coating into the resin. The normal load was constant during the test (on a distance of 4 mm, with a speed of 10mm/min) and was increased step by step between the tests: 5N, 10N, 15N, 20N. The tests data were recorded during the process, including: normal load, friction forces, friction coefficient, penetration and residual depth of the indenter. After the tests, the scratch scars were observed using both an optic microscope (at 185x) and SEM (HV = 20kV, 500x, WD = 15mm, LFDetector). Based on previous researches [4,9,10-4], there were measured the geometric values of the resulted cone-shaped fracture: width (a), cone length (b), projected area ( $A=(axb)/2$ ), which is considered the most characteristic comparison factor, since it demonstrated a proportional relationship with the scratching load.

### 3. Results and discussions

#### 3.1. Microstructures and mechanical properties

The microstructures of the investigated coatings cross section are presented in figure 2a, 3a (etched surface with nital). There were also analyzed using the line-chemical analysis in order to emphasize the homogenous distribution of chemical elements distribution (see figure 2b, 3b).

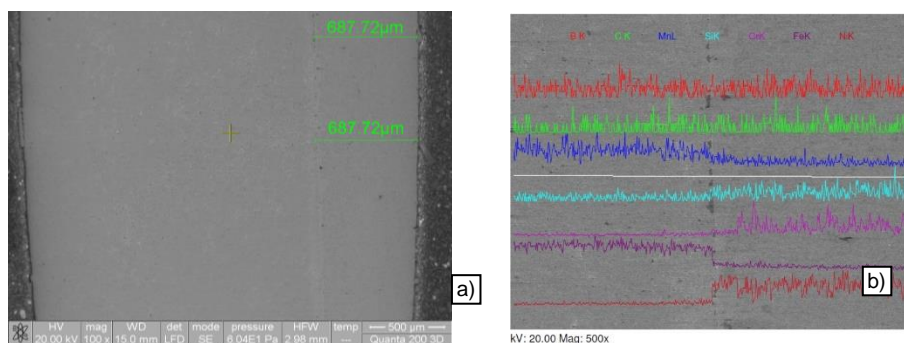


Fig. 2. Typical SEM images for 1060-00 coating: a) coating cross-section, c) line-chemical analysis.

The coatings microstructure is typical for the thermal sprayed category, having a lamellar structure composed of molten splats, unmelted particles, oxides layers and characteristic defects: small cracks, pores. The coatings thickness varied from 500 - 800μm and the estimated mean porosity was about 1%.

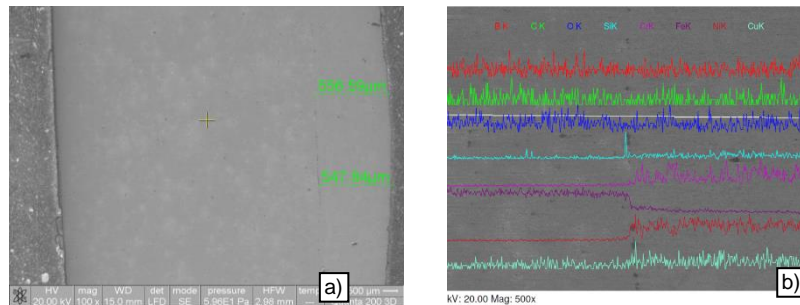


Fig. 3. Typical SEM images for 1355-20 coating: a) coating cross-section, c) line-chemical analysis.

From the microindentation tests conducted on the three samples result the microhardness values and Young modulus values, which are synthesized in Table 2. It could be noticed that the microhardness of coatings was in the expected limits, with a uniformity of measurements in case of 1355-20 coating.

Table 2. Microindentation tests results

Coating type	Microhardness (GPa)			
	1	2	3	Mean value
1060-00	4,76	5,28	5,82	5,28
1355-20	5,38	5,15	5,42	5,32
JK 586	5,29	4,99	5,87	5,38
Young's modulus (GPa)				
1060-00	108,5	118,8	119,9	115,7
1355-20	100	108	107	105
JK 586	88,87	87,6	81,4	85,9

### 3.2. Scratch tests

#### 3.2.1. Surface scratch tests

The results of the scratch tests indicate a good repeatability of the wear and friction results. The scratch scars aspects of coatings are presented in figures 4,5,6.

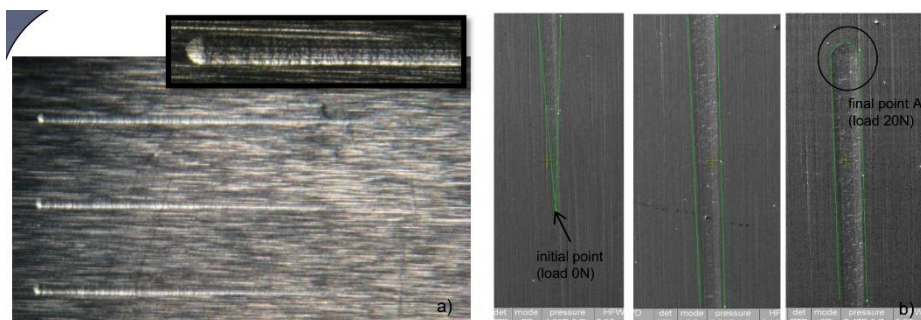


Fig.4. PLST scars on 1060-00 coating.

a) scratch scars (optic, 20x), b) scratch scars (SEM image, 100x).

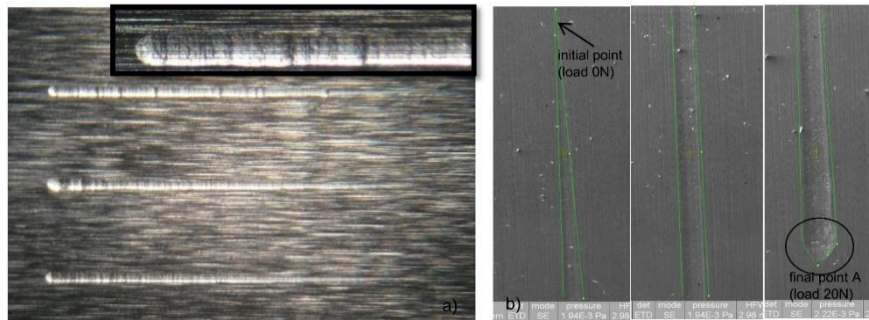


Fig.5. PLST scars on 1355-20 coating. a) scratch scars (optic, 20x), b) scratch scars (SEM image, 100x),

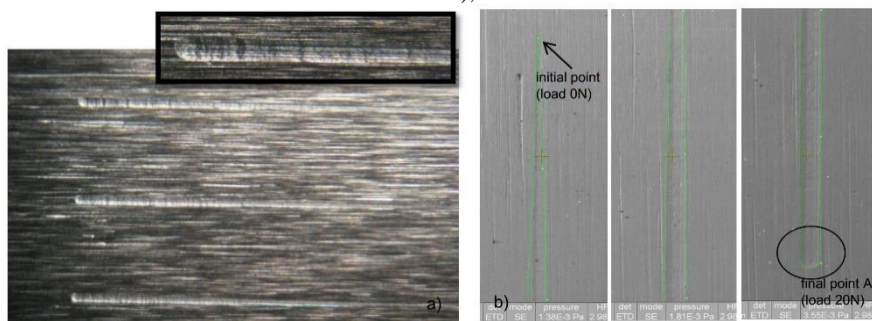


Fig.6. PLST on JK-586 coating. a) scratch scars (optic, 20x), b) scratch scars (SEM image, 100x),

The final point of each scratch scar was observed and analyzed using chemical-line type analysis with the EDAX-module on SEM, as it is presented in figures 7,8,9.

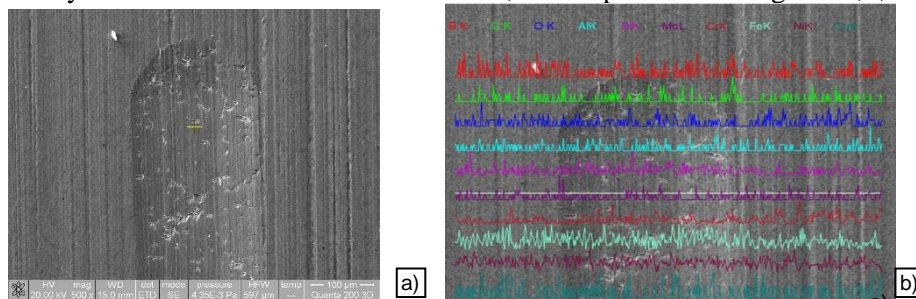


Fig.7. 1060-00 coating: a)scratch scar morphology (500x), b) chemical-line type analysis.

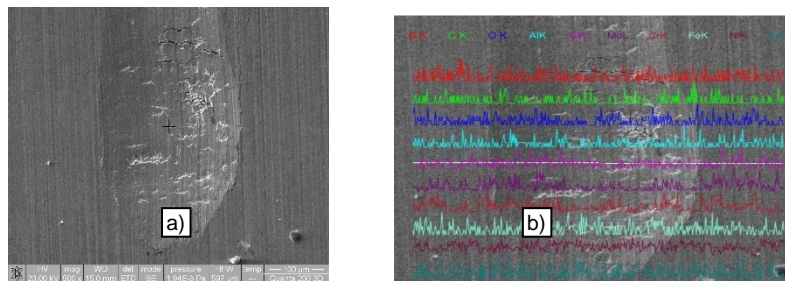


Fig.8. 1355-20 coating: a) scratch scar morphology (500x), b) chemical-line type analysis.

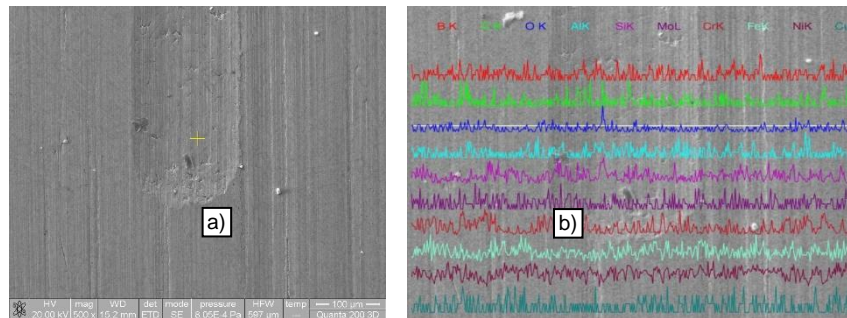


Fig. 9. JK 586 coating:  
a) scratch scar morphology (500x), b) chemical-line type analysis.

The depth of wear scars for the three coatings were measured and compared. The general tendency was the same for all three coating types: the wear rate increased with the normal load. The scar depths at half distance and at the final point are presented in Table 3.

Table 3. Scratch scars depth.

Coating type	Depth at half distance			Depth at final point		
	1 $\mu\text{m}$	2 $\mu\text{m}$	3 $\mu\text{m}$	1 $\mu\text{m}$	2 $\mu\text{m}$	3 $\mu\text{m}$
1060-00	6 $\mu\text{m}$	6 $\mu\text{m}$	6 $\mu\text{m}$	11 $\mu\text{m}$	15 $\mu\text{m}$	15 $\mu\text{m}$
1355-20	10 $\mu\text{m}$	8 $\mu\text{m}$	9 $\mu\text{m}$	13 $\mu\text{m}$	14 $\mu\text{m}$	12 $\mu\text{m}$
JK 586	5 $\mu\text{m}$	6 $\mu\text{m}$	6 $\mu\text{m}$	8 $\mu\text{m}$	8 $\mu\text{m}$	8 $\mu\text{m}$

Figure 10 presents, for exemplification, the wear scar profile at the maximum load measured for 1355 coating.

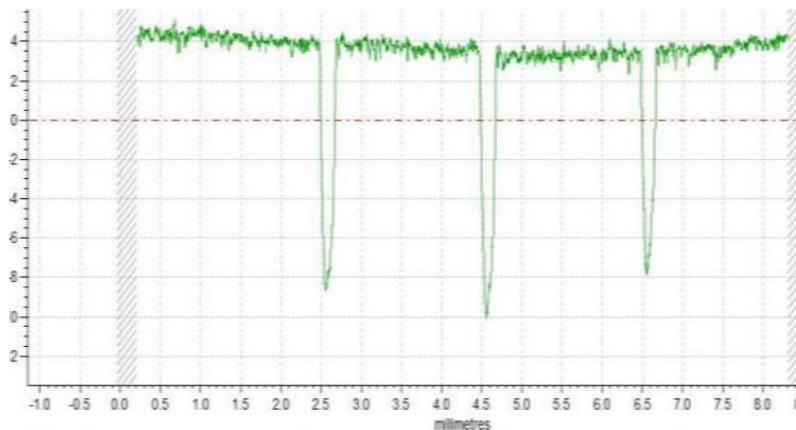


Fig.10. Wear scar profile of 1355 coating at maximum load (20N).

### 3.2.2. Cross-section scratch test

The projected cone areas resulted after the scratch tests conducted on the cross-sections were observed using OM, the depth and length of each cone was measured

and the cone surface was calculated. Fig. 11 presents the scratch scars on coating 1355-20, for all the loads (5N, 10N, 15N, 20N).

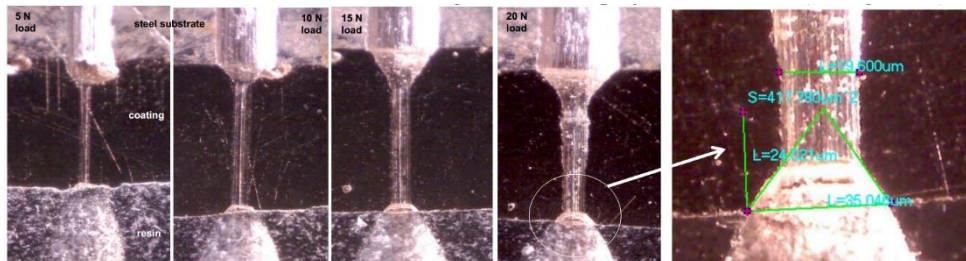


Fig.11. Cross-section scratch scars of 1355-20 coating at different loads (optical, detail B at 185x).

The results show that the projected cone area increased once with the scratching load. For all the samples, the cone originated in the coating, so the cohesion bond strength could be characterized. Figure 12 shows the morphology of cone produced at maximum load on cross section of 1060 coating.

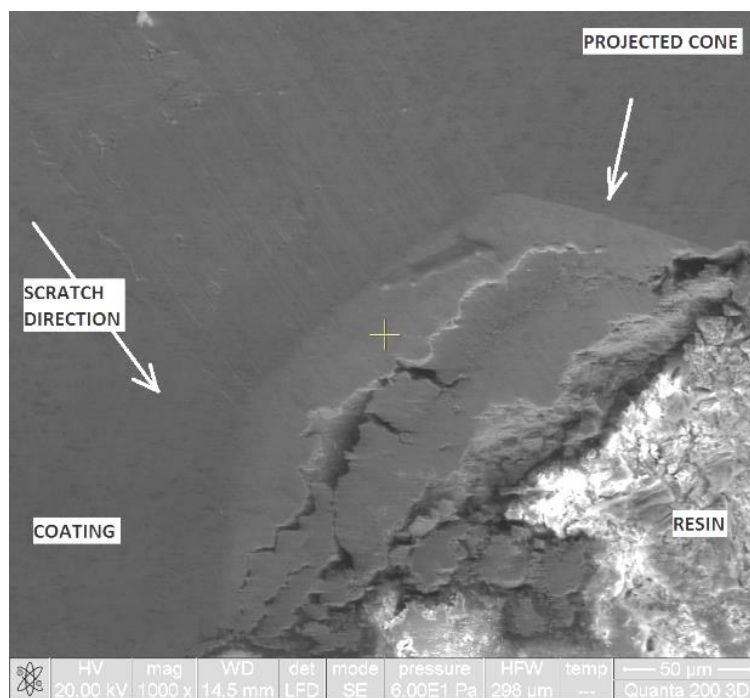


Fig.12. Typical SEM images of scratch cone produced on 1060-00 coating (1000x)

The main failure mechanism was the formation of three types of cracks, in the cross section: cracks present on the scratch tracks normal to scratch direction, cracks propagated from inside-out of the cone and cracks at the substrate – coating interface.

The calculated cone areas were comparatively analyzed in order to observe the differences of adhesion between the three coatings (see figure 13).

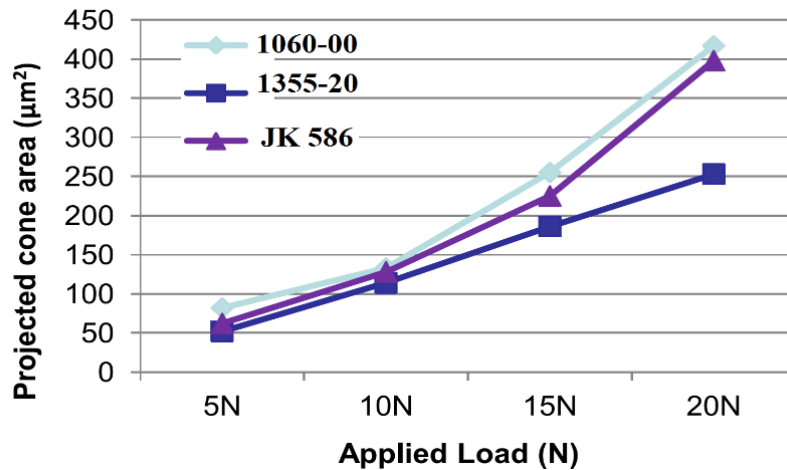


Fig.13. The variation of the projected cone area with the applied load.

It is noticeable that the projected cone area of sample 1 was larger than other coatings and the sample 3 possesses the smallest damage which means the highest cohesion bond strength.

#### 4. Conclusions

The scratch test represents an efficient and intuitive method, which could be used successfully for the characterization of cohesion bond strength of thermal-sprayed coatings.

The morphology of the scratch scars allows us to state that the wear mechanisms of thermal-sprayed coatings include the abrasive wear mechanism (caused by the particles that became detached during wear process) and also the fatigue wear mechanism (proved by the cracks and spalling observed on the worn coating surface).

The wear mechanisms produced on the coating surfaces and on the coatings cross-sections by the scratch tests are quite similar. They both represent coating failure under tensile stress, at the interface between splats, and both are relevant for characterization of coating cracks that originate in the coating defects and tensile residual stress.

#### References

- [1]. Lugscheider E., Barimani C., Eckert P., Eritt U., *Modeling of the APS plasma spray process*, Computational Materials Science, 7, 1996, p. 109–114.
- [2] Vencel A., Arostegui S., Favaro G., Zivic F., Mrdak M., Mitrović S. et al., *Evaluation of adhesion/cohesion bond strength of the thick plasma spray coatings by scratch testing on coatings cross-sections*, Tribology International, **44**, 2011, p. 1281-1288.

- [3] Rac A., *Basics of Tribology*, Faculty of Mechanical Engineering, University of Belgrade, Belgrade, 1991.
- [4] Tucker Jr. R.C., *Wear failures. In: Metals Handbook. Failure Analysis and Prevention*, vol. 11, p. 154–162, 9th edn. American Society for Metals, Metals Park, 1986.
- [5] Gates J.D., *Two-body and three-body abrasion: a critical discussion*, *Wear* 214, 1998, p. 139–146.
- [6] *Abrasive wear resistance*, *Ind. Lubr. Tribol.*, **43**, 1991, 14–26.
- [7] ASTM G 65-04 Standard Test Method for Measuring Abrasion Using the Dry Sand/Rubber Wheel Apparatus, 2004.
- [8] ASTM G 81-97a Standard Test Method for Jaw Crusher Gouging Abrasion Test, 2007.
- [9] ASTM G 105-02 Standard Test Method for Conducting Wet Sand/Rubber Wheel Abrasion Tests, 2007.
- [10] ASTM G 132-96 Standard Test Method for Pin Abrasion Testing, 2007.
- [11] ASTM G 174-04 Standard Test Method for Measuring Abrasion Resistance of Materials by Abrasive Loop Contact, 2004.
- [12] Hawk J.A., Wilson R.D., Tylczak J.H., Dogan O.N., *Laboratory abrasive wear tests: investigation of test methods and alloy correlation*, *Wear* 225–229, 1999, p. 1031–1042.
- [13] Sinha S.K., *180 years of scratch testing*, *Tribol. Int.*, **39**, 61, 2006.
- [14] Perry A.J., *The adhesion of chemically vapour deposited hard coatings to steel—the scratch test*, *Thin Solid Films*, **78**, 1981, p. 77–93.
- [15] Steinmann P.A., Hintermann H.E., *Adhesion of TiC and TiCN coatings on steel*, *J Vac Sci Technol* 1985, A3:2394–2400.
- [16] Valli J., *A review of adhesion test methods for thin hard coatings*, *J Vac Sci Technol*, 1986, A4:3001–3014.
- [17] Hintermann H.E., *Adhesion, friction and wear of thin hard coatings*, **100**, 1984, p. 381–397.
- [18] Perry A.J., *Scratch adhesion testing of hard coatings*. *Thin Solid Films*, 107, 1983, p. 167–180.
- [19] Bull S.J., Rickerby D.S., *New developments in the modelling of the hardness and scratch adhesion of thin films*, *Surf Coat Technol*, **42**, 1990, p. 149–164.
- [20] EN 1071-3:2002 Advanced Technical Ceramics—*Methods of Test for Ceramic Coatings—Part 3: Determination of Adhesive and Other Mechanical Failure Modes by a Scratch Test*, 2002.
- [21] Vencl A., Manic N., Popovic V., Mrdak M., *Possibility of the Abrasive Wear Resistance Determination with Scratch Tester*, *Tribol Lett*, **37**, 2010, p. 591–604.
- [22] Benjamin P., Weaver C., *Measurement of adhesion of thin films*, *Proc Roy Soc Lond, Ser A*, 254, 1960, p. 163–176.
- [23] Bull S.J., *Failure modes in scratch adhesion testing*, *Surf Coat Technol*, **50**, 1991, p. 25–32.
- [24] Bull S.J., *Spallation failure maps from scratch testing*, *Mater High Temp*, **13**, 1995, p. 169–174.
- [25] Bull S.J., *Failure mode maps in the thin film scratch adhesion test*, *Tribol Int*, **30**, 1997, p. 491–498.
- [26] Bull S.J., Rickerby D.S., Matthews A., Pace A.R., Leyland A., *Scratch adhesion testing of hard, wear-resistant coatings*, Broszeit E., Munz W.D., Oechsner H., Rie K.-T., Wolf G.K., editors. *Plasma surface engineering volume 2*, Oberursel: DGM Informations-gesellschaft, 1989, p. 1227–1235.
- [27] Steinmann P.A., Tardy Y., Hintermann H.E., *Adhesion testing by the scratch test method: the influence of intrinsic and extrinsic parameters on the critical load*, *Thin Solid Films*, **154**, 1987, p. 333–349.
- [28] Thouless M.D., *An analysis of spalling in the microscratch test*, *Eng Fract Mech*, **61**, 1998, p. 75–81.
- [29] Bull S.J., Berasetegui E.G., *An overview of the potential of quantitative coating adhesion measurement by scratch testing*. *Tribol. Int.*, **39**, 2006, p. 99–114.
- [30] Burnett P.J., Rickerby D.S., *The relationship between hardness and scratch adhesion*, *Thin Solid Films*, **154**, 1987, p. 403–416.
- [31] Gee M.G., *Low load multiple scratch tests of ceramics and hard metals*, 250, 2001, p. 264–281.
- [32] Helong Yu, Wei Zhang, Hongmei Wang, Yongming Guo, Min Wei, Zhanyong Song, Yong Wang, *Bonding and sliding wear behaviors of the plasma sprayed NiCrBSi coatings*, *Tribology International*, **66**, 2013, p. 105–113.